Chapter 10

Boiling Heat Transfer Inside Plain Tubes

(**This chapter was updated in 2007**)

SUMMARY: Evaporation inside plain tubes is described. Methods for evaporation in both vertical and horizontal tubes are covered. Some older design methods are first described and then the newest methods are presented. All these methods provide local predictions for flow boiling heat transfer coefficients for conditions in which the tube perimeter is completely or partially wet, but not for post-dryout heat transfer for mist flow. In addition, evaporation of mixtures is also addressed and a general prediction method is presented. Some of the methods also apply to evaporation in annuli formed by two concentric plain tubes. The recommended method for evaporation in vertical tubes is that of Steiner and Taborek (1992) while for horizontal tubes the method of choice is the updated version by Wojtan, Ursenbacher and Thome (2005a, 2005b) of the model of Kattan, Thome and Favrat (1998a, 1998b, 1998c).

10.1 Introduction

The various hydrodynamic conditions encountered when a liquid is evaporated in a confined channel, in this case round tubes, are described in this chapter together with methods to predict their heat transfer coefficients.

First of all, consider a vertical tube heated uniformly along its length (for example, by direct Joule heating of the tube by a DC power supply) at a relatively low heat flux with subcooled liquid entering the tube from the bottom and then completely evaporated over the length of the tube, as shown in Figure 10.1. While the liquid is being heated up to its saturation temperature at the local pressure at that height in the tube, the wall temperature initially is below that necessary for nucleation (zone A). Thus, the heat transfer process in zone A is subcooled, single-phase heat transfer to the liquid, which may be laminar or turbulent. Then, the wall temperature rises above the saturation temperature and boiling nucleation takes place in the superheated thermal boundary layer on the tube wall, such that subcooled flow boiling occurs in zone B with the vapor bubbles condensing as they drift into the subcooled core. The liquid then reaches its saturation temperature and saturated boiling in the form of bubbly flow begins in zone C. Saturated boiling continues through the slug flow regime (zone D), the annular flow regime (zone E) and then the annular flow regime with liquid entrainment in the vapor core (zone F).

At the end of zone F, the annular film is either dried out or sheared from the wall by the vapor, a point that is referred to as the onset of dryout or simply dryout. Above this point, mist flow in the form of entrained droplets occurs with a large increase in wall temperature for this instance of an imposed wall heat flux (zone G). The temperature of the continuous vapor-phase in zone G tends to rise above the saturation temperature and heat transfer is via four mechanisms: single-phase convection to the vapor, heat transfer to the droplets within the vapor, heat transfer to droplets impinging on the wall and thermal radiation from the wall to the droplets. Because of this non-equilibrium effect, droplets continue to exist in the vapor-phase beyond the point of x = 1, all the way to the beginning of zone H where all the liquid has been evaporated and heat transfer is by single-phase convection to the dry vapor.
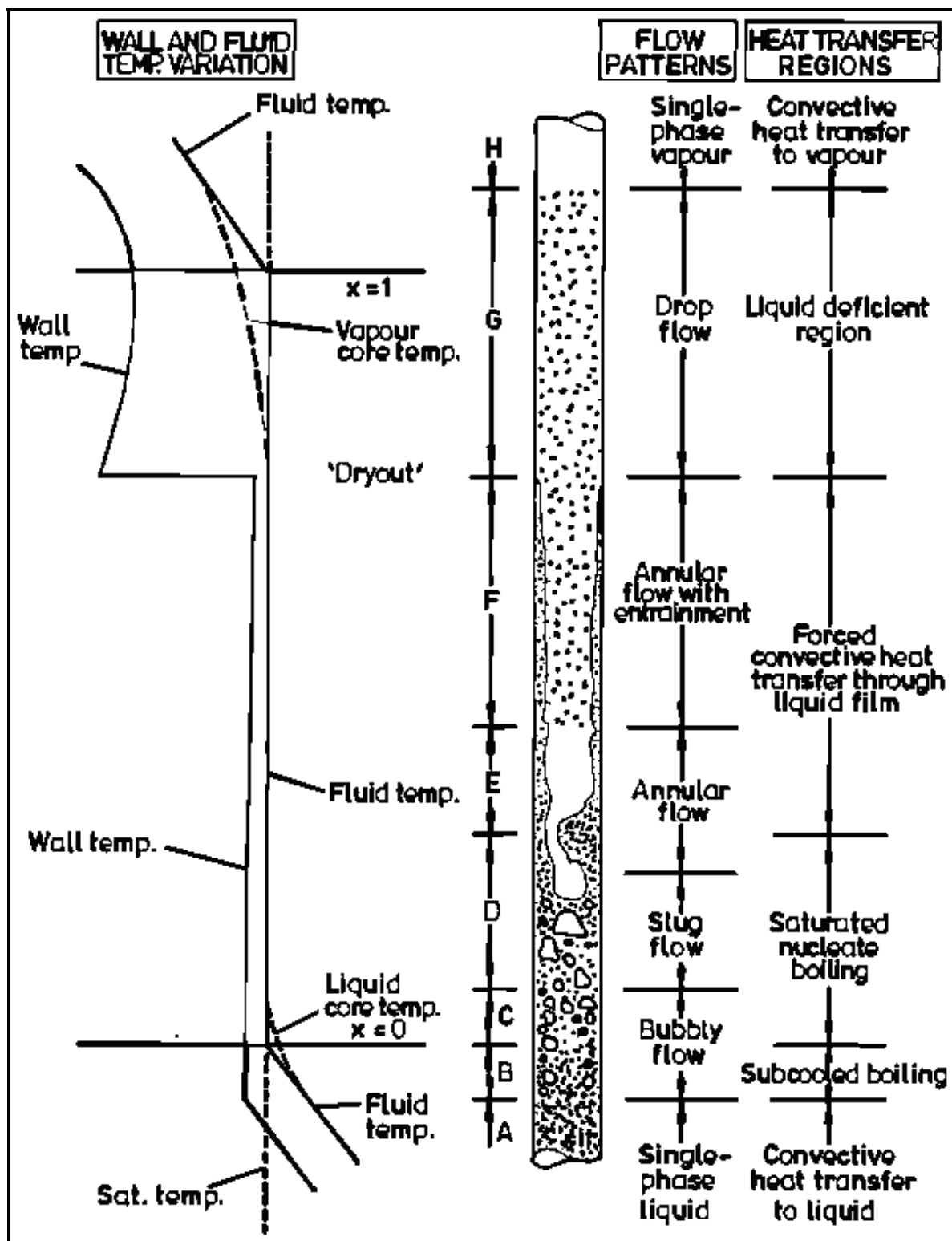
Figure 10.1. Heat transfer regions in convective boiling in a vertical tube from Collier and Thome (1994).

Figure 10.2 shows a "boiling map" for evaporation heat transfer, depicting qualitatively the progressive variation in the local heat transfer coefficient along a heated tube as the fluid evaporates. In essence, the map illustrates the variation in the heat transfer coefficient as a function of quality with increasing heat flux as the parameter, where the heat flux increases from (i) to (vii). At low heat fluxes the liquid deficient region is encountered at the dryout of the annular film. At higher heat fluxes, saturated film boiling is encountered by the process going through the departure from nucleate boiling (DNB), which is also commonly called the critical heat flux. Here, at least ideally, one can image that for film boiling an inverted annular flow occurs with the vapor forming an annular film and the liquid in the central core. As can be seen, at high heat fluxes it is possible to reach DNB under subcooled conditions. The heat transfer coefficients in the film boiling and liquid deficient regions are noticeably smaller than those in the wet wall region.
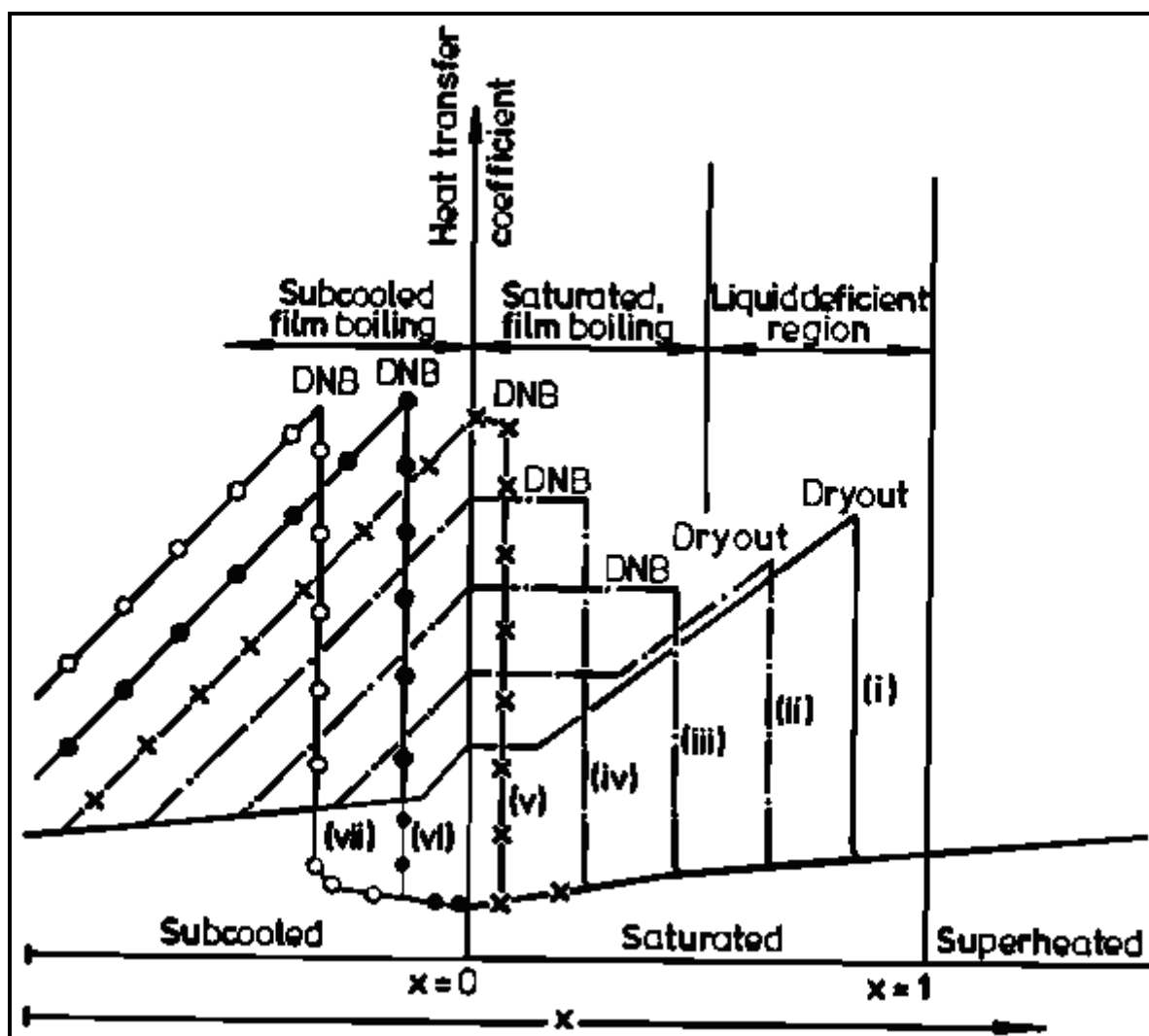

Figure 10.2. Boiling map of Collier and Thome (1994).

10.2 Two-Phase Flow Boiling Heat Transfer Coefficient

The local two-phase flow boiling heat transfer coefficient for evaporation inside a tube α_{tp} is defined as

$$\alpha_{tp} = \frac{q}{\left(T_{wall} - T_{sat}\right)} \qquad [10.2.1]$$

where q corresponds to the local heat flux from the tube wall into the fluid, T_{sat} is the local saturation temperature at the local saturation pressure p_{sat} and T_{wall} is the local wall temperature at the axial position along the evaporator tube, assumed to be uniform around the perimeter of the tube.

Flow boiling models normally consider two heat transfer mechanisms to be important: nucleate boiling heat transfer (α_{nb}) and convective boiling heat transfer (α_{cb}). Nucleate boiling under these conditions is similar to nucleate pool boiling except for any effect of the bulk flow on the growth and departure of the bubbles and the bubble induced convection process. The bubbles formed inside a tube may slide along the heated surface due to the axial bulk flow, and hence the microlayer evaporation process underneath the growing bubbles may also be affected. Convective boiling refers to the convective process between the heated wall and the liquid-phase. For instance, for annular flow without nucleate boiling in the liquid film, the convective heat transfer process can be envisioned as single-phase forced convection across the film with evaporation taking place at the liquid-vapor interface of the central core.

Before presenting flow boiling models, it is interesting to see how they can be compared and classified by the manner in which the heat transfer coefficients α_{nb} and α_{cb} are combined to obtain α_{tp} in the following power law format, typical of superposition of two thermal mechanisms upon one another:

$$\alpha_{tp} = \left[\left(\alpha_{nb}\right)^n + \left(\alpha_{cb}\right)^n\right]^{1/n} \qquad [10.2.2]$$

This power law format for α_{tp} is illustrated in Figure 10.3 for a fluid at a fixed pressure, mass flux, and vapor quality. Assuming that α_{cb} is not a function of heat flux, which is typical of most flow boiling prediction methods, α_{cb} is a horizontal line on this plot. Instead, α_{nb} is typically considered to be a function of heat flux but not mass velocity, and hence gives a nucleate pool boiling type of curve on this plot of heat transfer coefficient versus heat flux. Combining their values together using exponents of 1, 2, 3 and ∞ give the resulting variations in α_{tp}. Setting n = 1 results in a simple addition of the respective values. Chen (1963, 1966) used this approach but introduced a nucleate boiling suppression factor on α_{nb} and a two-phase multiplier on α_{cb}. Kutateladze (1961) proposed an asymptotic method with n = 2, where the value of α_{tp} tends to the larger of the two values. Steiner and Taborek (1992) more recently proposed using n = 3. Setting n = ∞ yields the larger of the two values, which is the approach proposed by Shah (1982).
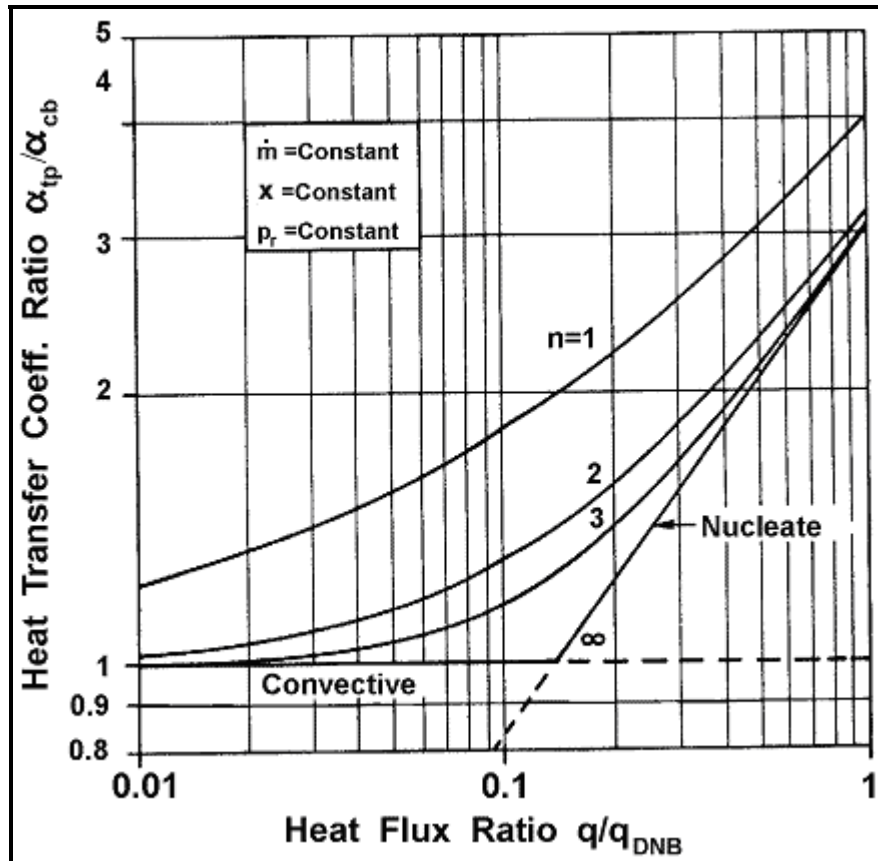
Figure 10.3. Power law representation of flow boiling models of Steiner and Taborek (1992).

10.3 Flow Boiling inside Vertical Plain Tubes

Convective evaporation in *vertical* tubes is discussed in this section, which is defined by the regions C, D, E and F in Figure 10.1. This process may either be forced convection, such as in a power boiler or a direct-expansion evaporator, or gravity driven as in a vertical thermosyphon reboiler. At high qualities and mass flow rates, the flow regime is normally annular. At relatively low flow rates at sufficient wall superheats, bubble nucleation at the wall occurs such that nucleate boiling is present within the liquid film. As the flow velocity increases and augments convection in the liquid film, the wall may be cooled below the minimum wall superheat necessary to sustain nucleation and nucleate boiling may thus be suppressed, in which case heat transfer is only by convection through the liquid film and evaporation occurs only at its interface.

Furthermore, at some threshold quality, the liquid film may dry out or become entrained in the high velocity vapor-phase, which results in poor heat transfer. This region is referred to as the post-dryout region, which will not be addressed in this chapter.

In nucleate pool boiling, heat transfer is a strong function of heat flux, by about $\alpha_{nb} \propto q^{0.7}$; instead in forced convective evaporation, heat transfer is less dependent on heat flux while its dependence on the local vapor quality and mass velocity appear as new and important parameters. Thus, both nucleate boiling and convective heat transfer must be taken into account to predict heat transfer data. Nucleate boiling tends to be dominant at low vapor qualities and high heat fluxes while convection tends to

dominate at high vapor qualities and mass velocities and low heat fluxes. For intermediate conditions, both mechanisms are often important.

The principal methods for predicting two-phase flow boiling heat transfer coefficients in vertical tubes are presented below. Generally speaking, the nucleate boiling coefficient α_{nb} is determined utilizing a nucleate *pool* boiling correlation from the literature or by proposing a new nucleate boiling term as part of the flow boiling correlation. Similarly, the convective heat transfer coefficient α_{cb} is typically related to what is sometimes referred to as the liquid only heat transfer coefficient α_L, which is determined with a single-phase turbulent flow heat transfer correlation, usually that of Dittus-Boelter (1930). Furthermore, these methods normally assume that the liquid fraction flowing in the channel, $\dot{m}(1-x)$, occupies the entire cross-section of the channel in the calculation of α_L.

10.3.1 Chen Correlation

Chen (1963, 1966) proposed the first flow boiling correlation for evaporation in vertical tubes to attain widespread use. He envisioned the local two-phase flow boiling coefficient α_{tp} to be the sum of the nucleate boiling contribution α_{nb} and the convective contribution α_{cb}:

$$\alpha_{tp} = \alpha_{nb} + \alpha_{cb} \qquad [10.3.1]$$

He surmised that the steeper temperature gradient in the liquid near the tube wall under forced convection conditions, relative to that in nucleate pool boiling, partially suppressed nucleation of boiling sites and hence reduced the contribution of nucleate boiling. On the other hand, he noted that the vapor formed by the evaporation process increased the liquid velocity and hence the convective heat transfer contribution tends to be increased relative to that of single-phase flow of the liquid. Hence, he formulated the following expression to account for these two effects:

$$\alpha_{tp} = \alpha_{FZ}S + \alpha_L F \qquad [10.3.2]$$

where

- the nucleate pool boiling correlation of Forster and Zuber (1955) is used to calculate the nucleate boiling heat transfer coefficient, α_{FZ};
- the nucleate boiling suppression factor acting on α_{FZ} is S;
- the turbulent flow correlation of Dittus-Boelter (1930) for tubular flows is used to calculate the liquid-phase convective heat transfer coefficient, α_L;
- and the increase in the liquid-phase convection due to the two-phase flow is given by his two-phase multiplier F.

The Forster-Zuber correlation gives the nucleate pool boiling coefficient as:

$$\alpha_{FZ} = 0.00122 \left[\frac{k_L^{0.79} c_{pL}^{0.45} \rho_L^{0.49}}{\sigma^{0.5} \mu_L^{0.29} h_{LG}^{0.24} \rho_G^{0.24}} \right] \Delta T_{sat}^{0.24} \Delta p_{sat}^{0.75} \qquad [10.3.3]$$

where the wall superheat ΔT_{sat} is the local temperature difference between the inner tube wall (T_{wall}) and the local saturation temperature (T_{sat}), such that $\Delta T_{sat} = (T_{wall} - T_{sat})$. The pressure difference Δp_{sat} is

obtained from the vapor pressures of the fluid at the wall temperature (p_{wall}) and at the saturation temperature (p_{sat}), such that $\Delta p_{sat} = (p_{wall} - p_{sat})$. In this expression, Δp_{sat} is in the units of N/m^2.

The liquid-phase convective heat transfer coefficient α_L is given by the Dittus-Boelter (1930) correlation for the fraction of liquid flowing alone in a tube of internal diameter d_i, i.e. using a mass velocity of $\dot{m}(1-x)$, as:

$$\alpha_L = 0.023 \, Re_L^{0.8} \, Pr_L^{0.4} \left(\frac{k_L}{d_i} \right)$$

[10.3.4]

where the liquid Reynolds number Re_L is:

$$Re_L = \frac{\dot{m}(1-x)d_i}{\mu_L}$$

[10.3.5]

and x is the local vapor quality and $\dot{m}$ is the total mass velocity of the liquid plus vapor in the tube of internal diameter d_i. Pr_L is the liquid Prandtl number defined as:

$$Pr_L = \frac{c_{pL}\mu_L}{k_L}$$

[10.3.6]

The two-phase multiplier F of Chen is:

$$F = \left(\frac{1}{X_{tt}} + 0.213 \right)^{0.736}$$

[10.3.7]

where the Martinelli parameter X_{tt} is used for the two-phase effect on convection, where X_{tt} is defined as:

$$X_{tt} = \left(\frac{1-x}{x} \right)^{0.9} \left(\frac{\rho_G}{\rho_L} \right)^{0.5} \left(\frac{\mu_L}{\mu_G} \right)^{0.1}$$

[10.3.8]

Note, however, that when $1/X_{tt} \leq 0.1$, F is set equal to 1.0. The Chen boiling suppression factor S is

$$S = \frac{1}{1 + 0.00000253 \, Re_{tp}^{1.17}}$$

[10.3.9]

This in turn is a function of his two-phase Reynolds number:

$$Re_{tp} = Re_L \, F^{1.25}$$

[10.3.10]

His fluid database included water in upflow and downflow (pressures from 0.55 to 34.8 bar) and methanol, cyclohexane, n-pentane, n-heptane and benzene, all in upflow at 1 bar. Most of the data were at low vapor qualities but the entire range covers values from 0.01 to 0.71. His correlation is applicable as long as the heated wall remains wet, i.e. up to the onset of dryout. Since the wall superheat ΔT_{sat} is

typically not known, an iterative calculation involving T_{wall} and p_{wall} is required when the heat flux q is specified.

10.3.2 Shah Correlation

The second flow boiling method for evaporation in vertical channels to reach a wide notoriety is that of Shah (1982), who proposed equations to implement his chart calculation method he proposed earlier. While he considered nucleate boiling and convective boiling to be the two important heat transfer mechanisms similar to Chen (1963, 1966), his method instead chooses the *larger* of the two, that is the larger of his nucleate boiling coefficient α_{nb} and his convective boiling coefficient α_{cb}, for the value of local two-phase flow boiling heat transfer coefficient α_{tp}. He proposed a method applicable to both vertical tubes and horizontal tubes. His vertical tube method is presented here, which begins by defining a dimensionless parameter N, which for vertical tubes at all values of the liquid Froude number Fr_L is:

$$N = C_0 \qquad [10.3.11]$$

and his factor C_o is determined from the local vapor quality and density ratio as:

$$C_0 = \left(\frac{1-x}{x}\right)^{0.8}\left(\frac{\rho_G}{\rho_L}\right)^{0.5} \qquad [10.3.12]$$

while the liquid Froude number is defined as:

$$Fr_L = \frac{\dot{m}^2}{\rho_L^2 g d_i} \qquad [10.3.13]$$

To characterize convection, the liquid-phase convective heat transfer coefficient α_L is determined from the liquid fraction of the flow, $\dot{m}(1-x)$, using the Dittus-Boelter (1930) correlation given in [10.3.4]. His convective boiling heat transfer coefficient α_{cb} is calculated as:

$$\frac{\alpha_{cb}}{\alpha_L} = \frac{1.8}{N^{0.8}} \qquad [10.3.14]$$

The effect of heat flux on nucleate boiling is characterized by the Boiling number, Bo, which is defined as:

$$Bo = \frac{q}{\dot{m}h_{LG}} \qquad [10.3.15]$$

representing the ratio of the actual heat flux to the maximum heat flux achievable by complete evaporation of the liquid. His parameter N is then used to determine the appropriate set of equations to use as follows:

When N > 1.0 and Bo > 0.0003. α_{nb} is calculated as below:

$$\frac{\alpha_{nb}}{\alpha_L} = 230 \, \text{Bo}^{0.5} \qquad\qquad\qquad [10.3.16]$$

When N > 1.0 and Bo < 0.0003. α_{nb} is calculated as below:

$$\frac{\alpha_{nb}}{\alpha_L} = 1 + 46 \, \text{Bo}^{0.5} \qquad\qquad\qquad [10.3.17]$$

When 1.0 > N > 0.1. α_{nb} is calculated as below:

$$\frac{\alpha_{nb}}{\alpha_L} = F_S \, \text{Bo}^{0.5} \exp(2.74N - 0.1) \qquad\qquad\qquad [10.3.18]$$

When N < 0.1. α_{nb} in the bubble suppression regime is calculated using the equation below:

$$\frac{\alpha_{nb}}{\alpha_L} = F_S \, \text{Bo}^{0.5} \exp(2.74N - 0.15) \qquad\qquad\qquad [10.3.19]$$

In the above equations, Shah's constant $F_S = 14.7$ when Bo > 0.0011 and $F_S = 15.43$ when Bo < 0.0011. The larger value of α_{nb} or α_{cb} is then taken for α_{tp}.

The most notable weakness of his method is that the only physical property in the boiling number Bo for characterizing nucleate boiling is the latent heat. Furthermore, the latent heat decreases with increasing pressure while α_{nb} typically increases with pressure.

Shah also applied this method to evaporation in vertical annuli as follows. When the annular gap between the inner and outer tubes is greater than 4 mm, the equivalent diameter to use for d_i is the difference between the two diameters; when the gap is less than 4 mm, the equivalent diameter to use for d_i is the hydraulic diameter determined using only the heated perimeter.

10.3.3 Gungor-Winterton Correlations

A new form of the Chen flow boiling model was proposed by Gungor and Winterton (1986), who put together a large database of 3,693 points from the literature for water, refrigerants (R-11, R-12, R-22, R-113 and R-114) and ethylene glycol for mostly vertical upflows and some vertical downflows. Their local two-phase flow boiling coefficient α_{tp} is also the sum of the nucleate boiling contribution α_{nb} and the convective contribution α_{cb}, where their basic equation is

$$\alpha_{tp} = E\alpha_L + S\alpha_{nb} \qquad\qquad\qquad [10.3.20]$$

Again, α_L is calculated from the Dittus-Boelter (1930) correlation given by [10.3.4] using the local liquid fraction of the flow, $\dot{m}(1-x)$, while their nucleate pool boiling coefficient is obtained with the Cooper (1984b) nucleate pool boiling equation:

$$\alpha_{nb} = 55 p_r^{0.12} \left(-0.4343 \ln p_r\right)^{-0.55} M^{-0.5} q^{0.67} \qquad\qquad\qquad [10.3.21]$$

The above equation is *dimensional* and gives the heat transfer coefficient in W/m²K. The heat flux q must be introduced in W/m². M is the molecular weight and p_r is the reduced pressure, which is the ratio of the saturation pressure p_{sat} to the critical pressure p_{crit}. Their two-phase convection multiplier E is a function of the Martinelli parameter and also the heat flux via the Boiling number:

$$E = 1 + 24000 Bo^{1.16} + 1.37 \left(\frac{1}{X_{tt}} \right)^{0.86} \qquad [10.3.22]$$

where X_{tt} and Bo have been defined earlier. Their boiling suppression factor S is

$$S = \left[1 + 0.00000115 E^2 Re_L^{1.17} \right]^{-1} \qquad [10.3.23]$$

with Re_L based on ṁ(1-x). Compared to their database, this method gave a mean deviation of ±21.4% compared to ±57.7% for the Chen (1963, 1966) correlation and ±21.9% for the Shah (1982) correlation. Hence, as the Shah correlation was not developed using this database, this comparison gives a good independent credibility of its accuracy. Using the same equivalent diameter definitions as Shah above, Gungor and Winterton predicted evaporation in vertical annuli to a mean error of ±29.4%.

Gungor and Winterton (1987) a year later proposed a newer, simpler version of this correlation based only on convective boiling:

$$\alpha_{tp} = E_{new} \alpha_L \qquad [10.3.24]$$

Their new two-phase convection multiplier E_{new} is:

$$E_{new} = 1 + 3000 Bo^{0.86} + 1.12 \left(\frac{x}{1-x} \right)^{0.75} \left(\frac{\rho_L}{\rho_V} \right)^{0.41} \qquad [10.3.25]$$

where Bo has been defined earlier and α_L is calculated as before. The accuracy was similar to their earlier correlation and this version has been recommended in Thome (1997a) as the better of the two compared to flow boiling data for R-134a.

10.3.4 Steiner-Taborek Asymptotic Model

Natural limitations to flow boiling coefficients. Before presenting a new prediction method, Steiner and Taborek (1992) stated that the following limits should apply to evaporation in vertical tubes:

- For heat fluxes below the threshold for the onset of nucleate boiling (q < q_{ONB}), only the convective contribution should be counted and not the nucleate boiling contribution.
- For very large heat fluxes, the nucleate boiling contribution should dominate.
- When x = 0, α_{tp} should be equal to the single-phase liquid convective heat transfer coefficient when q < q_{ONB} but α_{tp} should correspond to that plus α_{nb} when q > q_{ONB}.
- When x = 1.0, α_{tp} should equal the vapor-phase convective coefficient α_{Gt} (the forced convection coefficient with the total flow as vapor), assuming no liquid mist still exists in the flow at these conditions.
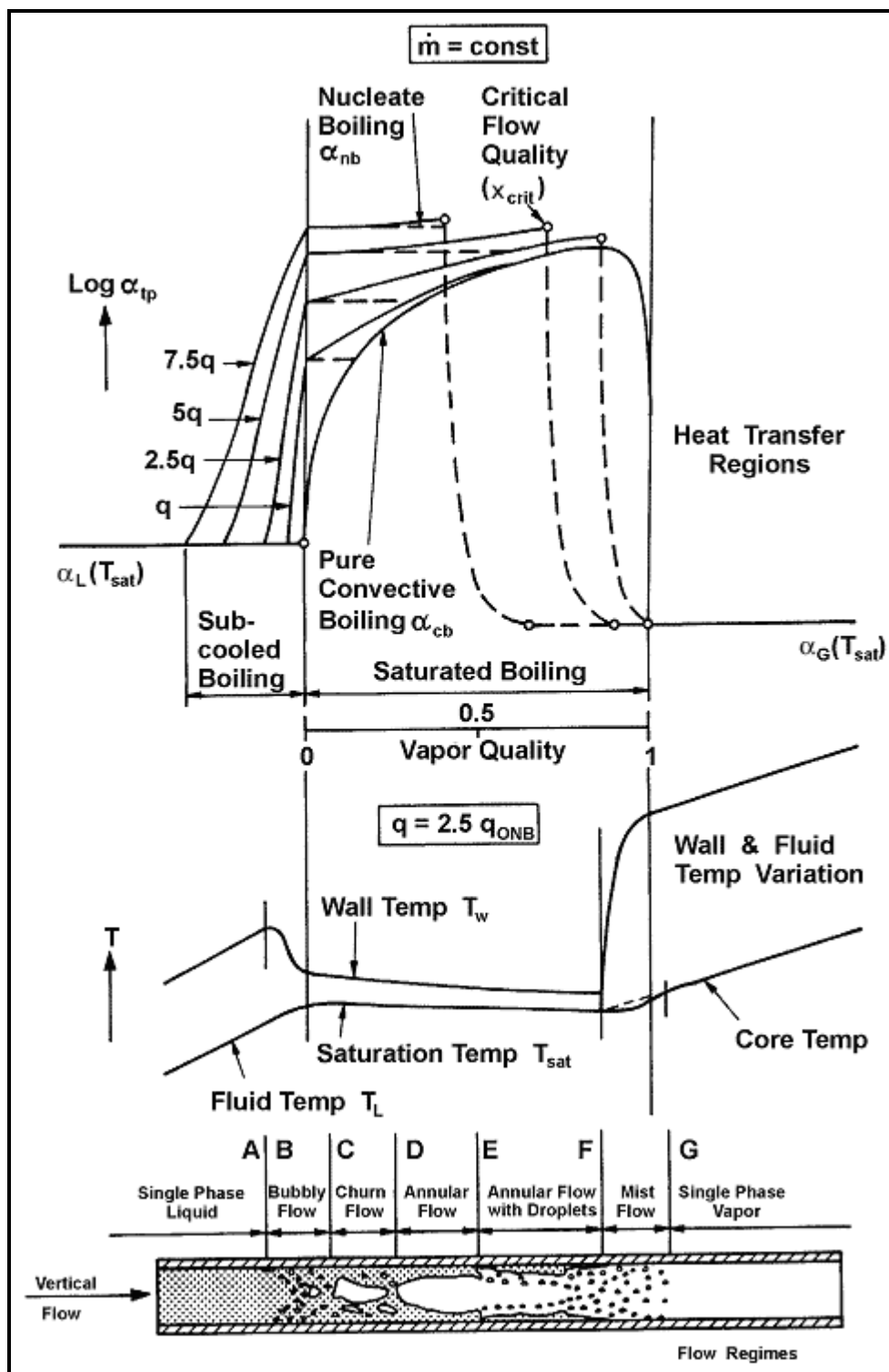
Figure 10.4. Boiling process in vertical tube according to Steiner-Taborek (1992).

Figure 10.4 illustrates the evolution of the heat transfer coefficient for evaporation in vertical tubes according to these limitations, which are further explained as follows:

- **Region A-B**. Before point A, only single-phase convection to the subcooled liquid occurs. Between points A and B, only liquid-phase convection occurs if $q < q_{ONB}$ while subcooled boiling occurs if $q > q_{ONB}$. In subcooled boiling, bubbles grow and collapse near the tube wall, which increases heat transfer.

- **Region B-C-D**. When $q < q_{ONB}$, only convective evaporation occurs as indicated by the "pure convective boiling" curve. When $q > q_{ONB}$, both nucleate and convective boiling contributions are present and are superimposed. The horizontal dashed lines are the nucleate boiling coefficient at the particular heat flux. The solid curves are the superimposed contribution of nucleate boiling and convective boiling, that is α_{tp}. The flow pattern passes through the bubbly flow and churn flow regimes as shown in the bottom diagram.

- **Region D-E-F**. When $q < q_{ONB}$, the process continues along the "pure convective boiling" curve up to the onset of dryout at high vapor qualities approaching 1.0. When $q > q_{ONB}$, the annular flow regime is reached, characterized by a thin turbulent annular liquid layer on the tube wall and a central vapor core, and continues up to the critical vapor quality x_{crit} reached where the annular film dries out.

- **Region F-G**. At x_{crit} the liquid film becomes unstable due to interfacial shear and adhesion forces. In the mist flow regime, the heat transfer mechanisms change completely, where heat is now transferred by vapor-phase convection, by evaporation of the entrained liquid droplets within the superheated vapor, by impingement of droplets on the wall and by radiation. (Note: the Steiner-Taborek model does *not* predict the dashed lines of the mist flow regime when $x > x_{crit}$).

Flow boiling model. Based on the above premises, Steiner and Taborek (1992) proposed a comprehensive evaporation model for vertical tubes. Their local flow boiling coefficient is obtained from an asymptotic approach using an exponent n equal to 3 as:

$$\alpha_{tp} = \left[\left(\alpha_{nb,o} F_{nb}\right)^3 + \left(\alpha_{Lt} F_{tp}\right)^3\right]^{1/3} \qquad [10.3.26]$$

In this expression, the parameters are as follows:

- $\alpha_{nb,o}$ is the local nucleate pool boiling coefficient at a reference heat flux q_o at the reduced pressure p_r equal to 0.1;
- F_{nb} is the nucleate boiling correction factor (but is *not* a boiling suppression factor, which is not required in an asymptotic model);
- α_{Lt} is the local liquid-phase forced convection coefficient based on the *total* flow as liquid (not on the liquid fraction of the flow as in the above methods) and is obtained with the Gnielinski (1976) correlation and not the Dittus-Boelter (1930) correlation;
- F_{tp} is the two-phase multiplier that accounts for enhancement of liquid convection by the higher velocity of a two-phase flow compared to single-phase flow of the liquid in the channel.

The Gnielinski correlation for obtaining α_{Lt} is:

$$\frac{\alpha_{Lt} d_i}{k_L} = \frac{\left(f_L/8\right)\left(Re_{Lt} - 1000\right)Pr_L}{1 + 12.7\left(f_L/8\right)^{1/2}\left(Pr_L^{2/3} - 1\right)} \qquad [10.3.27]$$

The Fanning friction factor, f_L, for the liquid is:

$$f_L = \left[0.7904 \ln\left(Re_{Lt}\right) - 1.64\right]^{-2} \qquad [10.3.28]$$

This expression is valid when $4000 < Re_{Lt} < 5000000$ and $0.5 < Pr_L < 2000$ for single-phase flows. The total mass velocity of liquid plus vapor is used for evaluating the liquid Reynolds number, so that Re_{Lt} is:

$$Re_{Lt} = \frac{\dot{m}d_i}{\mu_L} \qquad [10.3.29]$$

The two-phase multiplier F_{tp} is for convective evaporation, which will occur if $x < x_{crit}$ and $q > q_{ONB}$ or over the entire range of x if $q < q_{ONB}$. For applications where $x < x_{crit}$ at the tube exit and $q > q_{ONB}$, such as power boilers and thermosyphon reboilers, the following equation is used:

$$F_{tp} = \left[\left(1-x\right)^{1.5} + 1.9x^{0.6}\left(\frac{\rho_L}{\rho_G}\right)^{0.35}\right]^{1.1} \qquad [10.3.30]$$

This expression covers (ρ_L/ρ_G) from 3.75 to 5000 and converges to 1.0 as x goes to 0. x_{crit} is often assumed to occur at about 0.5 for these applications.

When $q < q_{ONB}$, only pure convective evaporation is present, extending from $x = 0.0$ to $x = 1.0$. At the limiting case at $x = 1.0$, the value of α_{tp} corresponds to α_{Gt}, which is the forced convection coefficient with the total flow as all vapor. The Gnielinski correlation is also used for obtaining α_{Gt}:

$$\frac{\alpha_{Gt}d_i}{k_G} = \frac{(f/8)\left(Re_{Gt} - 1000\right)Pr_G}{1 + 12.7(f/8)^{1/2}\left(Pr_G^{2/3} - 1\right)} \qquad [10.3.31]$$

The Fanning friction factor for the vapor, f_G, is:

$$f_G = \left[0.7904 \ln\left(Re_{Gt}\right) - 1.64\right]^{-2} \qquad [10.3.32]$$

The total mass velocity of liquid plus vapor is used for evaluating the vapor Reynolds number, so that Re_{Gt} is:

$$Re_{Gt} = \frac{\dot{m}d_i}{\mu_G} \qquad [10.3.33]$$

For this case, the following expression is used for F_{tp}:

$$F_{tp} = \left\{\left[\left(1-x\right)^{1.5} + 1.9x^{0.6}\left(1-x\right)^{0.01}\left(\frac{\rho_L}{\rho_G}\right)^{0.35}\right]^{-2.2} + \left[\left(\frac{\alpha_G}{\alpha_L}\right)x^{0.01}\left(1 + 8(1-x)^{0.7}\right)\left(\frac{\rho_L}{\rho_G}\right)^{0.67}\right]^{-2}\right\}^{-0.5}$$

$$[10.3.34]$$

This expression covers fluids with values of (ρ_L/ρ_G) from 3.75 to 1017. The terms with exponents of 0.01 make this expression go to its proper limits at $x = 0$ and $x = 1$.

The minimum heat flux for determining the onset of nucleate boiling q_{ONB} is given by the following expression using the liquid-phase heat transfer coefficient α_{Lt}:

$$q_{ONB} = \frac{2\sigma T_{sat}\alpha_{Lt}}{r_o\rho_G h_{LG}}$$

[10.3.35]

In this expression, σ is the surface tension, T_{sat} is the saturation temperature in Kelvin, r_o is the critical nucleation radius for a boiling site in meters and h_{LG} is the latent heat of vaporization. The recommended value for r_o is 0.3×10^{-6} m. For $q > q_{ONB}$, nucleate boiling is present in the flow boiling process but below this threshold it is not.

The nucleate boiling coefficient α_{nb} is determined here with a method similar to the nucleate pool boiling method of Gorenflo (1993) but the method below is *not* exactly the same. The *standard* nucleate boiling coefficients for the Steiner-Taborek flow boiling correlation $\alpha_{nb,o}$ are given in Table 10.1 at the following standard conditions: a reduced pressure of $p_r = 0.1$, a mean surface roughness of $R_{p,o} = 1$ μm and the heat flux q_o equal to the value listed for each fluid. The nucleate boiling correction factor F_{nb} includes the effects of reduced pressure, heat flux, tube diameter, surface roughness and a residual molecular weight correction factor on $\alpha_{nb,o}$ as follows:

$$F_{nb} = F_{pf}\left(\frac{q}{q_o}\right)^{nf}\left(\frac{d_i}{d_{i,o}}\right)^{-0.4}\left(\frac{R_p}{R_{p,o}}\right)^{0.133}F(M)$$

[10.3.36]

The pressure correction factor F_{pf}, valid for $p_r < 0.95$, accounts for the increase in the nucleate boiling coefficient with increasing pressure:

$$F_{pf} = 2.816\,p_r^{0.45} + \left\{3.4 + \left[\frac{1.7}{1-p_r^7}\right]\right\}p_r^{3.7}$$

[10.3.37]

The nucleate boiling exponent, nf, on the normalized heat flux term is:

$$nf = 0.8 - 0.1\exp(1.75p_r)$$

[10.3.38]

The above expression is for all fluids except cryogens (nitrogen, oxygen, etc.), where it is

$$nf = 0.7 - 0.13\exp(1.105p_r)$$

[10.3.39]

The standard tube reference diameter $d_{i,o}$ is 0.01 m, i.e. 10 mm. The standard value of the surface roughness is $R_{p,o} = 1$ μm (typical of industrial tubes and the default value if R_p is unknown) and the surface roughness term covers values of R_p from 0.1 to 18 μm. The residual molecular weight correction factor is in terms of the liquid molecular weight M (valid for $10 < M < 187$):

$$F(M) = 0.377 + 0.199\ln(M) + 0.000028427M^2$$

[10.3.40]

The maximum value of F(M) is 2.5, even when the expression gives a larger value. For cryogenic liquids H_2 and He, the values of F(M) are specifically 0.35 and 0.86, respectively.

Their method is based on an extensive database containing 10,262 data points for water and an additional 2345 data points for four refrigerants (R-11, R-12, R-22 and R-113), seven hydrocarbons (benzene, n-pentane, n-heptane, cyclo-hexane, methanol, ethanol and n-butanol), three cryogens (nitrogen, hydrogen and helium) and ammonia. It is currently regarded as the most accurate vertical tube boiling correlation available for pure fluids. However, it is difficult to extend its use to mixtures since there is no simple way to determine the values of $\alpha_{nb,o}$ for mixtures.

Table 10.1. Standard nucleate flow boiling coefficients of Steiner and Taborek (1992) for $\alpha_{nb,o}$ in W/m^2 K at p_r = 0.1 for q_o in W/m^2 and $R_{p,o}$ = 1 μm with p_{crit} in bar.

Fluid	p_{crit}	M	q_o	$\alpha_{nb,o}$
Methane	46.0	16.04	20000	8060
Ethane	48.8	30.07	20000	5210
Propane	42.4	44.10	20000	4000
n-Butane	38.0	58.12	20000	3300
n-Pentane	33.7	72.15	20000	3070
Isopentane	33.3	72.15	20000	2940
n-Hexane	29.7	86.18	20000	2840
n-Heptane	27.3	100.2	20000	2420
Cyclohexane	40.8	84.16	20000	2420
Benzene	48.9	78.11	20000	2730
Toluene	41.1	92.14	20000	2910
Diphenyl	38.5	154.2	20000	2030
Methanol	81.0	32.04	20000	2770
Ethanol	63.8	46.07	20000	3690
n-Propanol	51.7	60.10	20000	3170
Isopropanol	47.6	60.10	20000	2920
n-Butanol	49.6	74.12	20000	2750
Isobutanol	43.0	74.12	20000	2940
Acetone	47.0	58.08	20000	3270
R-11	44.0	137.4	20000	2690
R-12	41.6	120.9	20000	3290
R-13	38.6	104.5	20000	3910
R-13B1	39.8	148.9	20000	3380
R-22	49.9	86.47	20000	3930
R-23	48.7	70.02	20000	4870
R-113	34.1	187.4	20000	2180
R-114	32.6	170.9	20000	2460
R-115	31.3	154.5	20000	2890
R-123	36.7	152.9	20000	2600
R-134a	40.6	102.0	20000	3500
R-152a	45.2	66.05	20000	4000
R-226	30.6	186.5	20000	3700
R-227	29.3	170.0	20000	3800
RC318	28.0	200.0	20000	2710

Fluid	p_{crit}	M	q_o	$\alpha_{nb,o}$
R-502	40.8	111.6	20000	2900
Chloromethane	66.8	50.49	20000	4790
Tetrachloromethane	45.6	153.8	20000	2320
Tetrafluoromethane	37.4	88.00	20000	4500
Helium I £	2.275	4.0	1000	1990
Hydrogen (para)	12.97	2.02	10000	12220
Neon	26.5	20.18	10000	8920
Nitrogen	34.0	28.02	10000	4380
Argon	49.0	39.95	10000	3870
Oxygen	50.8	32.00	10000	4120
Water	220.6	18.02	150000	25580
Ammonia	113.0	17.03	150000	36640
Carbon Dioxide +	73.8	44.01	150000	18890
Sulfur Hexafluoride	37.6	146.1	150000	12230

£ Physical properties at $p_r = 0.3$ rather than 0.1;
+ Calculated with properties at T_{crit}.

10.4 Flow Boiling inside Horizontal Plain Tubes

Flow patterns formed during the generation of vapor in horizontal evaporator tubes are shown in Figure 10.5 taken from Collier and Thome (1994). The schematic representation of a horizontal tubular channel heated by a uniform low heat flux and fed with liquid just below the saturation temperature for a relatively low inlet velocity illustrates the sequence of flow patterns that might be observed. Asymmetric distributions of the vapor and liquid phases due to the effects of gravity introduce new complications compared to vertical upflow. Important points to note from a heat transfer standpoint are the possibility of complete drying or intermittent drying of the tube wall around part of the tube perimeter, particularly in slug and wavy flow and for annular flow with partial dryout. For example, in annular flow the film is thicker at the bottom than at the top, meaning the dryout tends to begin at the top and progressively increases around the perimeter of the tube in the direction of flow. In wavy flow, the top of the tube may be intermittently dry if the waves wash the top of the tube or always dry if they do not. These waves leave behind thin films of liquid that may or may not evaporate completely before the arrival of the next wave. The more widely quoted methods for predicting two-phase flow boiling heat transfer coefficients inside plain horizontal tubes are presented below.
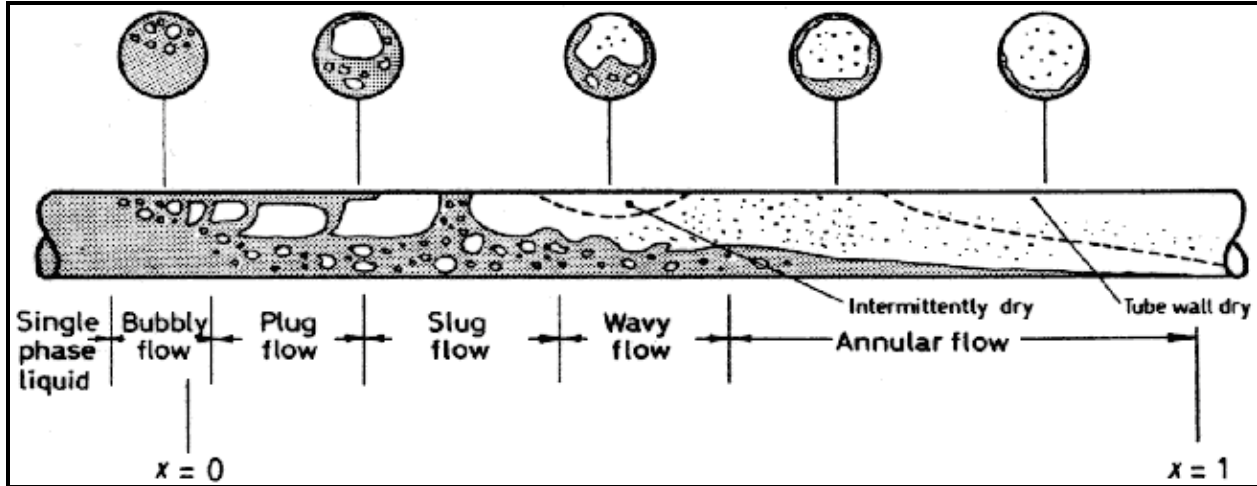
Figure 10.5. Flow patterns during evaporation in a horizontal tube from Collier and Thome (1994).

10.4.1 Vertical Tube Methods Applied to Horizontal Tubes

Many of the methods for predicting local flow boiling heat transfer coefficients in *horizontal* plain tubes are adaptations of *vertical* tube methods to horizontal test data, such as those of Shah (1982), Gungor and Winterton (1986, 1987), Klimenko (1988), Kandlikar (1990) and Wattelet et al. (1994). For instance, Shah (1982) made the following adjustments to his vertical tube method presented earlier. He set a threshold between stratified and non-stratified flow using the liquid Froude number Fr_L, defined as:

$$Fr_L = \frac{\dot{m}^2}{\rho_L^2 g d_i}$$
[10.4.1]

For $Fr_L < 0.04$, the flow is stratified and above 0.04 the flow is non-stratified. When $Fr_L > 0.04$, his vertical tube method is used without change with $N = C_o$. When $Fr_L < 0.04$, instead, the value of N is modified by the liquid Froude number Fr_L as:

$$N = 0.38 Fr_L^{-0.3} C_o$$
[10.4.2]

This correction has the tendency to reduce the two-phase flow boiling heat transfer coefficient at low mass velocities but leaves them unchanged at large mass velocities. It does not however account for the effect of vapor quality on the transition from stratified to non-stratified flow. Gungor and Winterton (1986) followed his example, setting their threshold value a little higher at $Fr_L < 0.05$. When $Fr_L > 0.05$, their vertical tube method is used without change but when $Fr_L < 0.05$, their factor E is corrected as follows

$$E_2 = Fr_L^{(0.1-2Fr_L)}$$
[10.4.3]

Thus, thus new parameter E_2 is applied as a multiplier to E in their method. Their boiling suppression factor S, is similarly multiplied by the another correction factor

$$S_2 = \left(Fr_L\right)^{1/2}$$
[10.4.4]

These two corrections again have the tendency to reduce the two-phase flow boiling heat transfer coefficient at low mass velocities but leaves them unchanged at large mass velocities. Kandlikar (1990) also set his stratification threshold at $Fr_L = 0.05$. Noting the difference in the trends in their heat transfer coefficients, Wattelet et al. (1994) classified their data as annular or stratified flow and set their stratification threshold to a much larger value of $Fr_L = 0.25$. It is worth emphasizing, however, that the liquid Froude number Fr_L is not a reliable approach for predicting the onset of stratification, as shown in a direct comparison to experimental flow observations for various refrigerants by Kattan, Thome and Favrat (1995a). This threshold criterion is in fact off by as much as 10 to 16 times in numerous instances! Hence, the above methods do not tend to predict heat transfer in stratified types of flow reliably nor accurately.

Never the less, the methods mentioned above do tend to predict heat transfer reasonably well in the annular flow regime. Their shortcomings can be summarized as follows:

- They only recognize stratified and non-stratified flows but not the different flow patterns occurring in horizontal flow boiling, and they tend to poorly predict the threshold from unstratified to stratified flow;
- Their local boiling coefficients plotted versus local vapor quality at a fixed heat flux q, that is a plot of α_{tp} vs. x, often do not represent the experimental trends nor the slope in α_{tp} vs. x;
- They do not account for the onset of dryout in annular flow at high vapor qualities and hence these methods are incapable of predicting the sharp peak in α_{tp} vs. x found in many experimental data sets nor do they predict the subsequent sharp decline in α_{tp} after the onset of dryout at the top of the tube in annular flows at high vapor qualities. Hence, they often overpredict heat transfer in this region by 100% to 300% or more;
- They attempt to model annular flow by modifying a *tubular* flow correlation (Dittus-Boelter) as opposed to modelling the liquid film using a *film* flow approach.

The foregoing flow boiling correlations therefore do not qualify as general methods, especially for stratified types of flows nor for local conditions with partial dryout on the top perimeter of the tube. In their favor, however, these methods are comprised of a small set of equations and are easy to quickly implement.

10.4.2 Local Flow Pattern Evaporation Model of Kattan-Thome-Favrat

A more phenomenological approach, incorporating the local two-phase flow structure as a function of the local flow pattern, has been proposed by Kattan, Thome and Favrat (1998a, 1998b, 1998c). Their method is based on their own two-phase flow pattern map for horizontal evaporating flows (described separately in the chapter on two-phase flow patterns). So far, their flow boiling model covers fully stratified flows, stratified-wavy flows, intermittent flows, annular flows and annular flows with partial dryout. Plug and slug flows are classified as intermittent flows, in which the tube wall is assumed to always remain wet by frequent passing of large amplitude waves that leave behind a liquid film on the top of the tube. Intermittent flows have a very complex flow structure and were for simplicity modelled as annular flows with reasonable success. Similarly, annular flow with partial dryout is classified as a form of stratified-wavy flow and is modelled as such. Heat transfer in bubbly and mist flow regimes are not currently addressed in their model.

Figure 10.6 depicts the simplified two-phase flow structures they assumed to represent the fully-stratified, stratified-wavy and annular flow regimes. For fully-stratified flow, the liquid flows in the bottom of the tube with essentially an undisturbed flat horizontal interface with the vapor above; taking the same wetted perimeter as for the flat surface, it is assumed that the equivalent heat transfer process is to a liquid film of thickness δ whose cross-sectional area A_L is equal to that of the stratified area of the liquid. For annular

flow (and intermittent flow), the liquid fraction is assumed to all be in the annular film on the tube wall, again designated by a film thickness δ. For stratified-wavy flow (and annular flow with partial dryout), the truncated annular ring varies around the perimeter of the tube from the lower fully-stratified limit up to the annular limit.
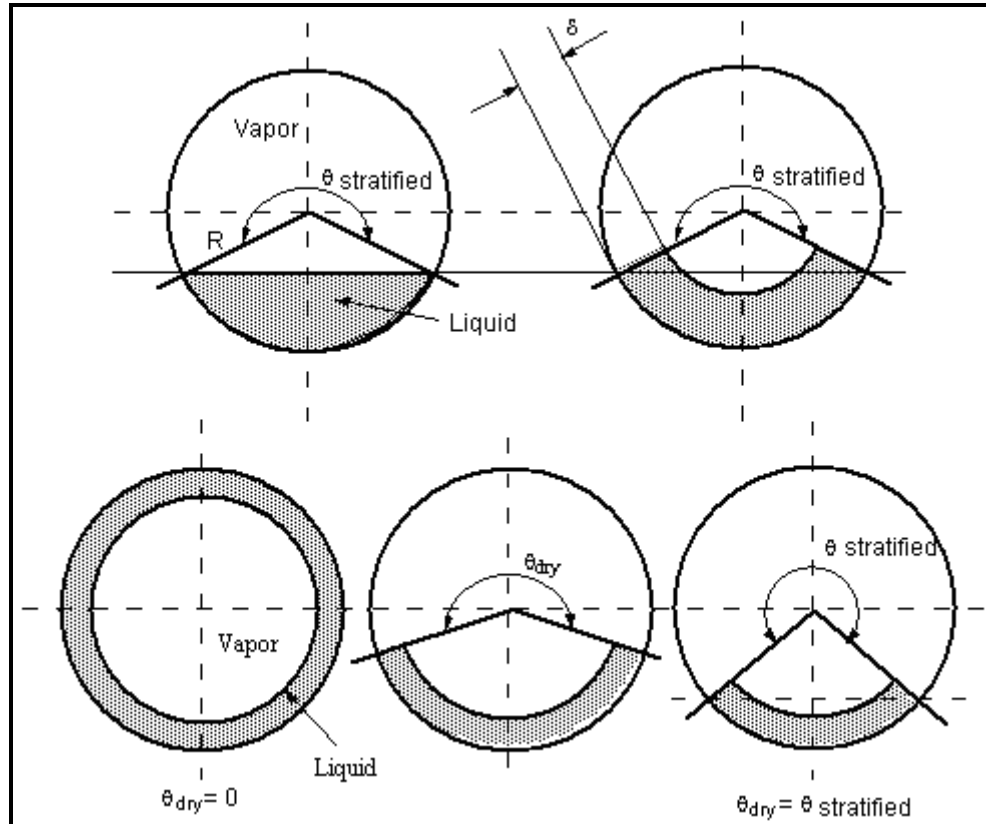

Figure 10.6. Geometric illustration of liquid and vapor areas, stratified and dry angles, and liquid film thickness in the flow boiling model.

The general equation for the local flow boiling coefficient α_{tp} for evaporation in a horizontal, plain tube in the Kattan-Thome-Favrat method for an internal tube diameter of d_i is:

$$\alpha_{tp} = \frac{d_i \theta_{dry} \alpha_{vapor} + d_i (2\pi - \theta_{dry}) \alpha_{wet}}{2\pi d_i}$$

[10.4.5]

The dry perimeter of the tube, if any, is given by the dry angle θ_{dry} and the heat transfer coefficient on this surface is α_{vapor}. On the wetted perimeter, the heat transfer coefficient is α_{wet}, which is obtained from an asymptotic expression that combines the nucleate boiling α_{nb} and convective boiling α_{cb} contributions using an exponent of three as:

$$\alpha_{wet} = \left(\alpha_{nb}^3 + \alpha_{cb}^3 \right)^{1/3}$$

[10.4.6]

The *dimensional* reduced pressure correlation of Cooper (1984b) is used to determine α_{nb}:

$$\alpha_{nb} = 55 p_r^{0.12} \left(-\log_{10} p_r \right)^{-0.55} M^{-0.5} q^{0.67}$$ [10.4.7]

The surface roughness in his expression has been set equal to his standard surface roughness factor (1.0 μm), such that the surface correction factor equals 1.0 and disappears from the above expression. In applying his correlation, α_{nb} is in W/m^2K, p_r is the reduced pressure, M is the liquid molecular weight and q is the heat flux at the tube wall in W/m^2. His multiplier of 1.7 for copper tubes is ignored.

Visualizing the annular ring of liquid more realistically as a *film* flow rather than as a *tubular* flow, the convective boiling heat transfer coefficient α_{cb} is predicted as follows:

$$\alpha_{cb} = 0.0133 \left[\frac{4\dot{m}(1-x)\delta}{(1-\varepsilon)\mu_L} \right]^{0.69} \left[\frac{c_{pL}\mu_L}{k_L} \right]^{0.4} \frac{k_L}{\delta}$$ [10.4.8]

where 0.0133 and 0.69 are empirical constants determined from their original database for five refrigerants and are generally applicable to other fluids for turbulent annular films. The term in the first bracket is the liquid film Reynolds number Re_L while the second bracket represents the liquid Prandtl number Pr_L. The mean liquid velocity in the cross-section of the tube occupied by the liquid is used in this definition of the liquid Reynolds number, which is a function of the vapor quality x, annular liquid film thickness δ, and vapor void fraction ε.

Assuming *tubular* flow on the dry perimeter of the tube at the mass velocity of the vapor, $\dot{m}x$, the vapor-phase heat transfer coefficient α_{vapor} is obtained with the Dittus-Boelter (1930) turbulent flow heat transfer correlation:

$$\alpha_{vapor} = 0.023 \left[\frac{\dot{m}x d_i}{\varepsilon \mu_G} \right]^{0.8} \left[\frac{c_{pG}\mu_G}{k_G} \right]^{0.4} \frac{k_G}{d_i}$$ [10.4.9]

The vapor Reynolds number Re_G in the first bracketed term is based on the mean vapor velocity in the cross-section of the tube occupied by the vapor.

The dry angle θ_{dry} around the top of the tube is the angle of the tube wall that is assumed to be constantly dry for stratified types of flows and annular flows with partial dryout. For annular and intermittent flows, the entire tube perimeter is always wet and hence θ_{dry} is equal to zero; thus for these latter two flow regimes, α_{tp} is equal to α_{wet} (intermittent flow is modelled as annular film flow for heat transfer purposes). In addition, k_L and k_G are the liquid and vapor thermal conductivities, c_{pL} and c_{pG} are the liquid and vapor specific heats, and μ_L and μ_G are the liquid and vapor dynamic viscosities. The total mass velocity of the liquid plus vapor through the tube is $\dot{m}$ and x is the local vapor quality. Methods for determining θ_{dry}, ε and δ are described below.

The vapor void fraction ε is predicted using the drift flux void fraction model of Rouhani-Axelsson (1970) for vertical tubes that was modified by Steiner (1993) for horizontal tubes:

$$\varepsilon = \frac{x}{\rho_G} \left\{ \left[1 + 0.12(1-x) \right] \left(\frac{x}{\rho_G} + \frac{1-x}{\rho_L} \right) + \frac{1.18}{\dot{m}} \left[\frac{g\sigma(\rho_L - \rho_G)}{\rho_L^2} \right]^{1/4} (1-x) \right\}^{-1}$$ [10.4.10]

where $\dot{m}$ is the total mass velocity of liquid and vapor, x is the local vapor quality, ρ_L and ρ_G are the liquid and vapor densities, and σ is the surface tension (all in SI units). The cross-sectional area of the tube occupied by the liquid-phase A_L is obtained using the cross-sectional void fraction ε as:

$$A_L = A(1 - \varepsilon)$$

[10.4.11]

where A is the total internal cross-sectional area of the tube. For the fully stratified flow regime as illustrated in Figure 10.6, the stratified angle θ_{strat} (in radians) of the liquid layer in the lower part of the tube is:

$$A_L = 0.5r_i^2[(2\pi - \theta_{strat}) - \sin(2\pi - \theta_{strat})]$$

[10.4.12]

The above equation is an implicit geometrical expression and is solved iteratively to find the value of the stratified angle θ_{strat} using the value of A_L where r_i is the internal radius of the tube. The dry angle θ_{dry} varies from its lower limit of $\theta_{dry} = 0$ for annular flow with complete wall wetting at the mass velocity $\dot{m}_{high}$ to its maximum value of $\theta_{dry} = \theta_{strat}$ for fully stratified flow at the mass velocity $\dot{m}_{low}$. The transition boundary from the intermittent and annular flow regimes to stratified-wavy flow $\dot{m}_{wavy}$ is used for $\dot{m}_{high}$ while $\dot{m}_{strat}$ is used for $\dot{m}_{low}$ (refer to the Kattan-Thome-Favrat flow pattern map in the respective chapter). To determine θ_{dry}, a simple linear interpolation between $\dot{m}_{high}$ and $\dot{m}_{low}$ is assumed when $x < x_{max}$ as illustrated in Figures 10.6 and 10.7:

$$\theta_{dry} = \theta_{strat} \frac{(\dot{m}_{high} - \dot{m})}{(\dot{m}_{high} - \dot{m}_{low})}$$

[10.4.13]

Thus, θ_{dry} changes as the values of $\dot{m}_{high}$ and $\dot{m}_{low}$ change with x in the above expression.
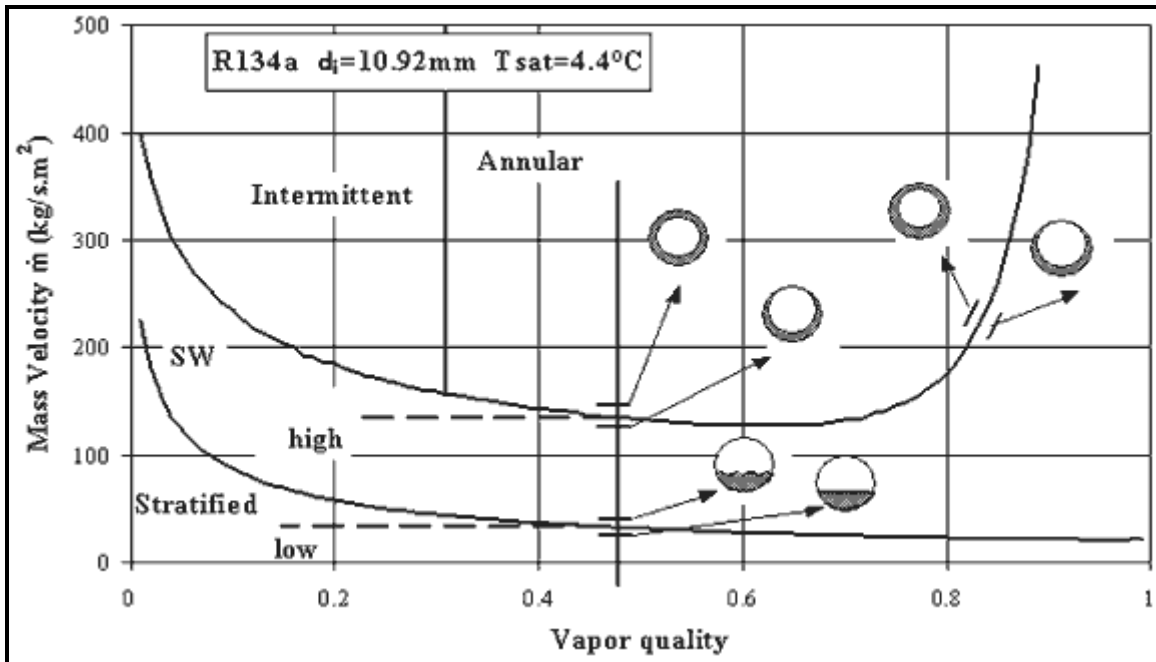

Figure 10.7. Two-phase flow pattern map showing low and high locations when $x < x_{max}$.

The annular liquid film thickness δ is determined by equating the cross-sectional area occupied by the liquid phase A_L for this particular void fraction and dry angle to the area of a truncated annular liquid ring, assuming the thickness δ is small compared to the tube radius r_i:

$$\delta = \frac{A_L}{r_i(2\pi - \theta_{dry})} = \frac{A(1-\varepsilon)}{r_i(2\pi - \theta_{dry})} = \frac{\pi d_i(1-\varepsilon)}{2(2\pi - \theta_{dry})} \qquad [10.4.14]$$

When $x > x_{max}$, an additional step is required to determine θ_{dry} as shown in Figure 10.8. Since $\dot{m}_{high}$ in this case passes the intersection of the $\dot{m}_{wavy}$ and $\dot{m}_{mist}$ curves, when $x > x_{max}$ there is no $\dot{m}_{wavy}$ curve for determining $\dot{m}_{high}$ and thus the dry angle θ_{dry} is prorated *horizontally*:

$$\theta_{dry} = (2\pi - \theta_{max})\frac{(x - x_{max})}{(1 - x_{max})} + \theta_{max} \qquad [10.4.15]$$

assuming that it varies linearly between the values of θ_{max} and 2π, the latter which is the upper limit at $x = 1$, and θ_{max} is determined from Equation (10.4.13) with $x = x_{max}$.
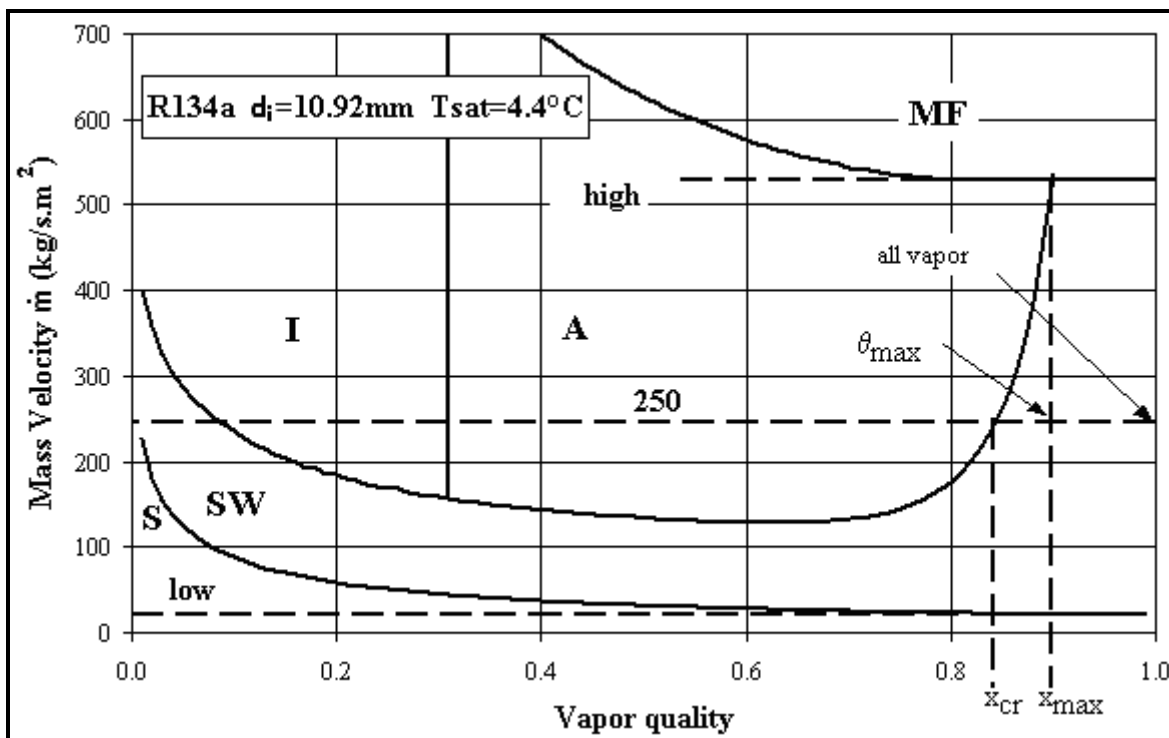

Figure 10.8. Dry angle θ_{dry} when $x > x_{max}$.

Zürcher, Thome and Favrat (1999) extended application of the Kattan-Thome-Favrat model to evaporation of ammonia for mass velocities as low as 16.3 kg/m²s (11773 lb/h ft²s), reduced pressures as low as 0.0085 and heat fluxes as high as 71.6 kW/m² (22700 Btu/h ft²) for stainless and carbon steel tubes. Overall, the Kattan-Thome-Favrat flow boiling model has so far been verified over the following range of conditions:

- $1.12 \le p_{sat} \le 8.9$ bar (16.2-129.0 psia);

- $0.0085 \leq p_r \leq 0.225$;
- $16.3 \leq \dot{m} \leq 500$ kg/m^{2}s (11,773-367,900 lb/h ft^{2}s);
- $0.01 \leq x \leq 1.0$;
- $440 \leq q \leq 71,600$ W/m^2 (140-22700 Btu/h ft^2);
- $17.03 \leq M \leq 152.9$ (not including values up to about 300 obtained with refrigerant-oil mixtures);
- $74 \leq Re_L \leq 20399$ and $1,300 \leq Re_G \leq 376,804$;
- $1.85 \leq Pr_L \leq 5.47$ (but Pr_L values up to 134 including tests with refrigerant-oil mixtures);
- $0.00016 \leq \mu_L \leq 0.035$ Ns/m^2 (0.16 to 35 cp, including results for refrigerant-oil mixtures);
- $10.9 \leq d_i \leq 16.0$ mm (0.43-0.63 in. but now being compared to a much wider range);
- Fluids: R-134a, R-123, R-502, R-402A, R-404A, R-407C and ammonia;
- Tube metals: copper, carbon steel and stainless steel.

For annular flows, its accuracy is similar to those of the Shah (1982), Jung et al. (1989), and Gungor-Winterton (1986, 1987) correlations, except that these latter methods do not know when annular flow exists nor do they get the correct slope in α_{tp} vs. x. When the flow is stratified-wavy, the Kattan-Thome-Favrat model is twice as accurate as the best of these other methods, even though these others have stratified flow threshold criteria and corresponding heat transfer correction factors. For x > 0.85 typical of direct-expansion evaporator applications, the Kattan-Thome-Favrat model is three times more accurate than the best of these other methods, which have standard deviations of ±80% or more.

Including the update to the wavy flow and stratified flow transition equations in the flow pattern map by Zürcher, Thome and Favrat (1999), Figure 10.9 presents the flow pattern map and heat transfer coefficients predicted by the above Kattan-Thome-Favrat heat transfer model. The simulation is for saturated n-butane at 60°C (140 °F) and 6.4 bar (92.8 psia), a heat flux of 15 kW/m^2 (4756 Btu/h ft^2), and an internal tube diameter of 19.86 mm (0.782 in.). The following comments can be made:

- All local heat transfer coefficients are *continuous* from one flow regime to another without any step changes in the values of α_{tp};
- For $\dot{m} = 20$ kg/m^{2}s (14716 lb/h ft^{2}s), *fully stratified flow* occurs at all values of x and α_{tp} declines monotonically with increasing x as the dry angle increases;
- For $\dot{m} = 60$ kg/m^{2}s (44150 lb/h ft^{2}s), *stratified-wavy flow* occurs at all x with a moderate peak in α_{tp} vs. x;
- For $\dot{m} = 200$ kg/m^{2}s (147160 lb/h ft^{2}s) and x $\leq$ 0.4, *intermittent flow* occurs with a moderate rise in α_{tp} vs. x;
- For $\dot{m} = 200$ kg/m^{2}s (147160 lb/h ft^{2}s) and 0.4 < x < 0.93, *annular flow* occurs with an increasing rise in α_{tp} vs. x as the annular film thins out up to the onset of dryout at x = 0.93;
- For $\dot{m} = 200$ kg/m^{2}s (14720 lb/h ft^{2}s) and x $\geq$ 0.93, *annular flow with partial dryout* (modelled as stratified-wavy flow) occurs with a sharp decline in α_{tp} vs. x.

Also, in this model the heat transfer coefficient goes to its natural limit at x = 1.0, i.e. single-phase turbulent flow of all the flow as vapor. However, for x = 0 the convective boiling heat transfer coefficient α_{cb} for liquid *film* flow does not go to its natural limit of the *tubular* value. Hence, when x = 0, α_{cb} should be obtained with either the Dittus-Boelter or Gnielinski correlation given earlier.
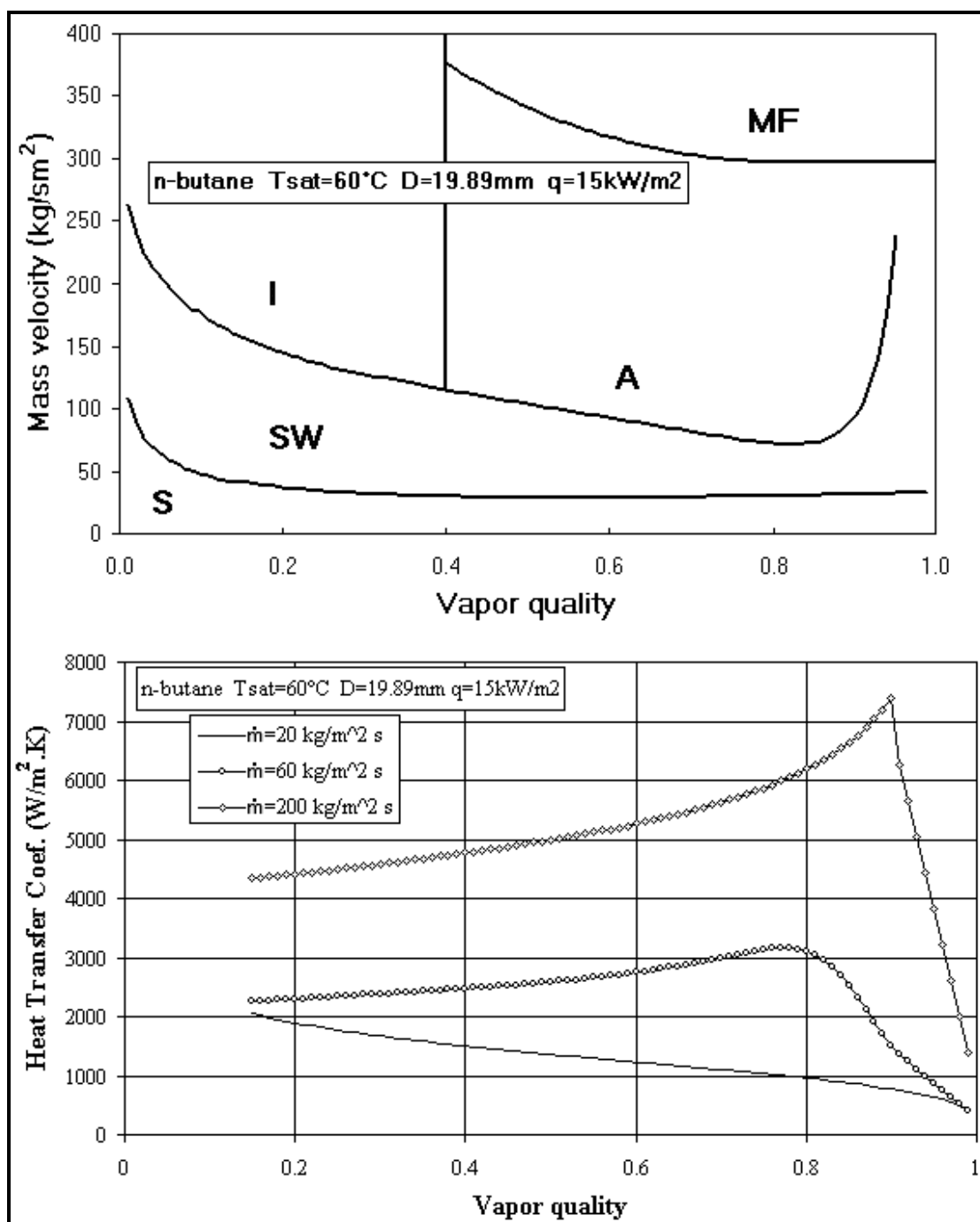
Figure 10.9. Flow pattern map and heat transfer for pure n-butane at 60°C using Kattan-Thome-Favrat model.

10.4.3 Evaporation of Mixtures

The Kattan-Thome-Favrat model was formulated as a general model for pure fluids, azeotropic mixtures and multi-component zeotropic mixtures. Multi-component zeotropic mixtures, i.e. mixtures with two or more components, experience a temperature glide during evaporation, such as the three-component mixture R-407C. The effect of liquid-phase mass transfer on the nucleate boiling contribution to flow

boiling was included by introducing the Thome (1989) mixture boiling equation into the Cooper correlation, whose analytical mass transfer resistance factor F_c for nucleate pool boiling of mixtures is a function of the boiling range ΔT_{bp}, i.e. the dew point temperature minus the bubble point temperature of the mixture at its local liquid composition. His factor F_c is:

$$F_c = \left\{ 1 + \left(\alpha_{id}/q \right) \Delta T_{bp} \left[1 - \exp\left(\frac{-q}{\rho_L h_{LG} \beta_L} \right) \right] \right\}^{-1}$$

[10.4.16]

In this expression, $F_c < 1.0$ for zeotropic mixtures since $\Delta T_{bp} > 0$ but $F_c = 1.0$ for pure fluids and azeotropes since for these fluids $\Delta T_{bp} = 0$. The nucleate boiling heat transfer coefficient for zeotropic mixtures is thus obtained by including F_c in the Cooper correlation to give:

$$\alpha_{nb} = 55 p_r^{0.12} \left(-\log_{10} p_r \right)^{-0.55} M^{-0.5} q^{0.67} F_c$$

[10.4.17]

where q is the total local heat flux and p_r and M are those of the liquid mixture. The mass transfer coefficient β_L is a fixed value of 0.0003 m/s based on comparisons to numerous experimental pool boiling studies by Thome and coworkers for hydrocarbon and aqueous mixtures with from two to five components. The ideal heat transfer coefficient α_{id} is first determined with [10.4.17] with F_c set equal 1.0. This method is valid for boiling ranges up to about 30 K (54°F) and hence covers many of the zeotropic refrigerant blends and hydrocarbon mixtures of industrial interest.

As an example of its application, Zürcher, Thome and Favrat (1998a) successfully compared the above method to their R-407C flow boiling data. The same approach has also been applied to the vertical tube boiling correlation of Gungor and Winterton (1986).

10.4.4 Instructions for Implementation of Kattan-Thome-Favrat Model

The Kattan-Thome-Favrat flow boiling model requires more steps than prior methods and the following is a step-by-step procedure for its implementation for a given tube internal diameter, specific design conditions (tube diameter, mass velocity, heat flux, pressure and vapor quality) and fluid physical properties. The steps are as follows:

1. Determine the local flow pattern corresponding to the local design condition using the Kattan-Thome-Favrat flow pattern map (refer to the chapter on flow pattern maps);
2. Calculate the local vapor void fraction ε;
3. Calculate the local liquid cross-sectional area A_L;
4. If the flow is annular or intermittent, determine δ with θ_{dry} set to 0;
5. If the flow is stratified-wavy (note that the flow pattern map classifies annular flow with partial dryout at the top of the tube as being stratified-wavy), iteratively calculate θ_{strat}, then the values of $\dot{m}_{high}$ and $\dot{m}_{low}$ at x are used to calculate θ_{dry} using the method for $x \leq x_{max}$ or $x > x_{max}$, and then δ is determined with this value of θ_{dry};
6. If the flow is fully stratified, iteratively calculate θ_{strat} and then determine δ setting θ_{strat} equal to θ_{dry};
7. Determine α_{cb};
8. Calculate α_{vapor} if part of the wall is dry;
9. If the fluid is a pure, single-component liquid or an azeotropic mixture, directly determine α_{nb} using the total local heat flux q;

10. If the fluid is a zeotropic mixture, determine α_{id}, F_c and then α_{nb};
11. Calculate α_{wet} using the values of α_{nb} and α_{cb};
12. Determine the local flow boiling coefficient α_{tp}.

10.4.5 Updated Version of Kattan-Thome-Favrat Model

The Kattan-Thome-Favrat flow boiling model has been updated by improvements to its flow pattern map in Wojtan, Ursenbacher and Thome (2005a) and to its heat transfer model in Wojtan, Ursenbacher and Thome (2005b). For changes to their diabatic two-phase flow pattern map, refer to Chapter 12. The improvements to the flow boiling heat transfer model are described below. Basically, changes to the heat transfer model were made to (*i*) incorporate the three new subzones of the stratified-wavy region that requires a new approach in the dry angle calculation, (*ii*) the annular flow zone has been modified by addition of a fixed nucleate boiling suppression factor to better reflect their experimental results, (*iii*) a mist flow heat transfer model has been added to cover that flow regime for which previously no method had been recommended, and (*iv*) a dryout region heat transfer method has been added for the region that separates the annular flow and stratified-wavy flow regimes from mist flow. The mist flow and dryout region heat transfer prediction methods of Wojtan, Ursenbacher and Thome (2005a, 2005b) are not described here as they are presented in Chapter 18.

The Kattan-Thome-Favrat model assumed a linear variation of the dry angle in stratified-wavy flow between 0 at $\dot{m}_{high}$ (that is $\dot{m}_{wavy}$) and θ_{strat} at $\dot{m}_{low}$ (that is $\dot{m}_{strat}$), as shown in expression [14.4.13]. Zürcher, Thome and Favrat (1999) did not make any changes in the heat transfer model in the stratified-wavy region even though that study showed that some experimental data points at low vapor qualities were clearly under predicted by the model of Kattan-Thome-Favrat model (the original model restricted itself to vapor qualities greater than 0.15). However, in an analogous model for condensation in horizontal tubes, Thome, El Hajal and Cavallini (2003) assumed a quadratic interpolation to calculate θ_{dry} rather than a linear interpolation:

$$\theta_{dry} = \theta_{strat} \left[\frac{\dot{m}_{high} - \dot{m}}{\dot{m}_{high} - \dot{m}_{low}} \right]^{0.5}$$

[10.4.18]

As noted above, in the Wojtan-Ursenbacher-Thome map and flow boiling model, the stratified-wavy region has been subdivided into three subzones (slug, slug/stratified-wavy and stratified-wavy) and these modifications result in an important change of the dry angle calculation. The following procedures are now utilized to find the dry angle in the three new subzones while still avoiding any jump in the heat transfer coefficient at any transition boundary.

Slug Regime (Slug). In this regime, the high frequency slugs are thought to maintain a continuous thin liquid film on the upper tube perimeter, meaning the entire tube perimeter always remains wet. Thus, similar to the intermittent and annular flow regime:

$$\theta_{dry} = 0$$

[10.4.19]

Stratified-Wavy Regime (SW). Based on their experimental flow boiling heat transfer data for this region, better agreement has been found using an exponent of 0.61 rather than 1.0 or 0.5 to capture the wetting effect of the side walls of the tube by the waves, such that:

$$\theta_{dry} = \theta_{strat} \left[\frac{\dot{m}_{high} - \dot{m}}{\dot{m}_{high} - \dot{m}_{low}} \right]^{0.61} \qquad [10.4.20]$$

Slug/Stratified-Wavy Regime (Slug+SW): In the slug/stratified-wavy zone, both low amplitude waves (which do not reach the top of the tube) and liquid slugs that wash the top of the tube and completely wet the tube perimeter are observed. With increasing vapor quality in this region, the slug frequency decreases and the small amplitude waves become dominant, as observed in Wojtan, Ursenbacher and Thome (2004) with their flow visualization/image processing results for cross-sectional void fractions. The slugs disappeared completely approximately at a vapor quality of x_{IA}. To capture this effect and to avoid a jump in the heat transfer coefficient at the boundaries of this regime, the following interpolation was proposed and applied when $x < x_{IA}$:

$$\theta_{dry} = \theta_{strat} \left(\frac{x}{x_{IA}} \right) \left[\frac{\dot{m}_{high} - \dot{m}}{\dot{m}_{high} - \dot{m}_{low}} \right]^{0.61} \qquad [10.4.21]$$

All presented modifications assure a smooth transition in the determination of dry angle between respective subzones and also a smooth transition in the heat transfer coefficient from subzone to subzone.

Three more modifications were made in Intermittent, Annular, Strafied and Stratified-Wavy flows (the later subdivided into subzones of Slug, SW+Slug, SW) compared to the original Kattan-Thome-Favrat flow boiling model:

- The liquid film thickness is now calculated as follows instead of using [10.4.14]:

$$\delta = \frac{d_i}{2} - \left[\left(\frac{d_i}{2} \right)^2 - \frac{2A_L}{2\pi - \theta_{dry}} \right]^{1/2} \qquad [10.4.22]$$

- When the liquid occupies more than one-half of the cross-section of the tube at low vapor quality, this expression would yield a value of $\delta > d_i/2$, which is not geometrically realistic. Hence, whenever [10.4.22] gives $\delta > d_i/2$, δ is set equal to $d_i/2$.

- θ_{strat} is calculated non-iteratively using the expression of Biberg (1999) with ε from [10.4.10]:

$$\theta_{strat} = 2\pi - 2 \left\{ \begin{array}{l} \pi(1-\varepsilon) + \left(\frac{3\pi}{2} \right)^{1/3} \left[1 - 2(1-\varepsilon) + (1-\varepsilon)^{1/3} - \varepsilon^{1/3} \right] \\ - \frac{1}{200}(1-\varepsilon)\varepsilon[1 - 2(1-\varepsilon)]\left[1 + 4\left((1-\varepsilon)^2 + \varepsilon^2 \right) \right] \end{array} \right\} \qquad [10.4.23]$$

A fixed value of a nucleate boiling suppression factor of S=0.8 was introduced to reduce the nucleate boiling contribution based on their database, so that [10.4.6] now becomes:

$$\alpha_{wet} = \left[(S\alpha_{nb})^3 + \alpha_{cb}^3 \right]^{1/3} \qquad [10.4.24]$$

After this modification, the new updated model predicted their experimental points more accurately, particularly for higher heat fluxes. It was also seen that the inception of dryout was better identified and that the new heat transfer model predicted the experimental heat transfer data more accurately for the dryout regime as well as for the mist flow regime.

Figure 10.10 shows a simulation of the Wojtan-Ursenbacher-Thome updated flow pattern map and flow boiling model for R-134a at a saturation temperature of 10°C, a mass velocity of 500 kg/m^{2}s and a heat flux of 7500 W/m^2 for a tube of 10 mm internal diameter. The black lines represent the flow pattern transition boundaries, the red line shows the variation in the predicted heat transfer coefficient and the dashed red line shows the process path. The heat transfer coefficient at a vapor quality of 0.5 is 6206 W/m^{2}K.
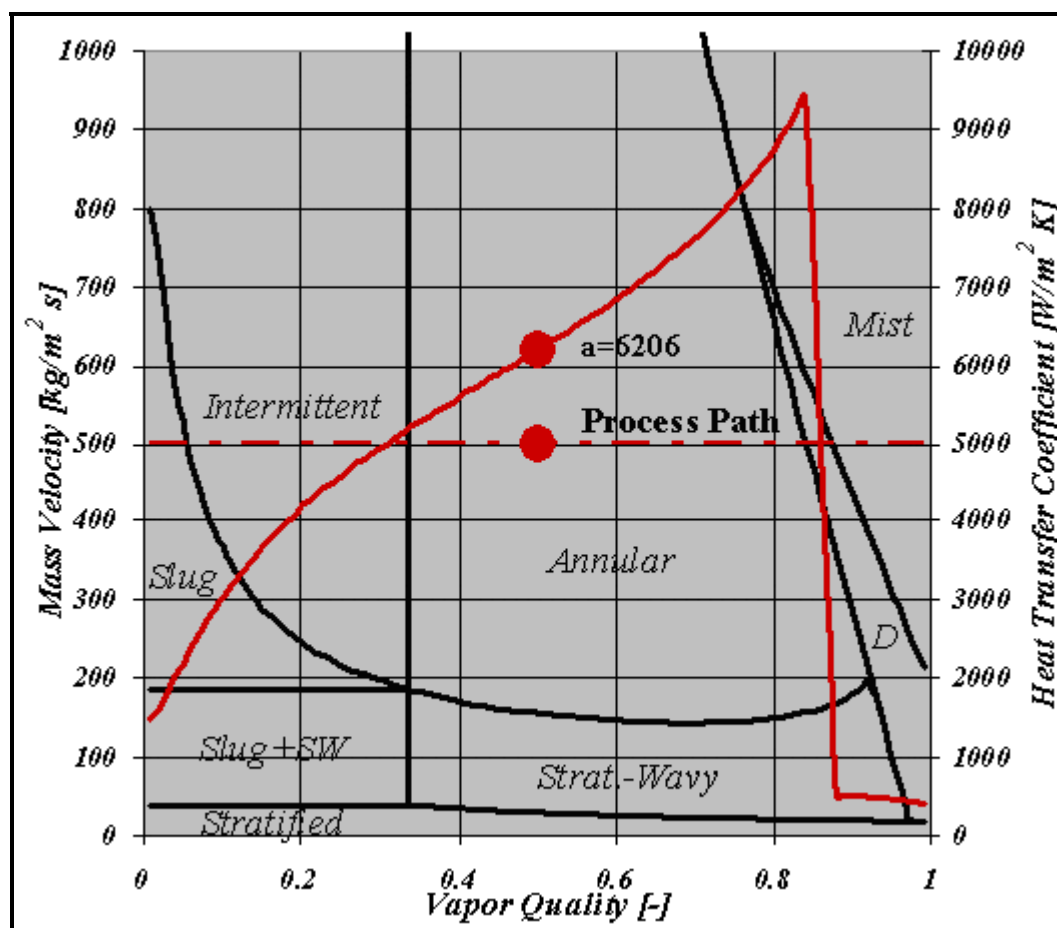

Figure 10.10. Simulation of Wojtan-Ursenbacher-Thome updated flow pattern map and flow boiling model for R-134a at a saturation temperature of 10°C, a mass velocity of 500 kg/m^{2}s and a heat flux of 7500 W/m^2 for a tube of 10 mm internal diameter.

10.5 Heat Transfer Measurements in Horizontal Tubes

Consider the following question. Is it appropriate to measure flow boiling heat transfer data in horizontal tubes using electrical heating (by direct resistance heating of the tube itself or with heated tapes wrapped on the tube)? That is a subject of some debate, where the current preference is to use counter-current hot

water heating. The following comments are pertinent: (i) for annular flow, the values of α_{tp} will be very similar, (ii) for all types of stratified flow, hot liquid heating induces a nearly uniform temperature boundary condition around the tube perimeter, which is similar to actual operation, while electrical heating creates circumferential heat conduction around the tube from the hot, dry-wall condition at the top to the colder, wet-wall condition at the bottom, yielding an unknown boundary condition, (iii) for annular flow with partial dryout on the top perimeter of the tube, electrical heating is also not advisable because of axial heat conduction along the test section.

In the past, electrical heating had the advantage of providing local heat transfer coefficients while hot water heating normally gave sectional average or what might be called "quasi-local" values for changes in vapor quality from 3-10% or more within the test zone. However, using hot fluid heating and a series of local hot fluid thermocouples to measure the hot fluid's temperature profile together with wall mounted thermocouples, a technique adopted by Kaul, Kedzierski and Didion (1996) and Zürcher, Thome and Favrat (1999), provides true local flow boiling heat transfer coefficients without resorting to electrical heating nor having to be satisfied with "quasi-local" data. Combining the temperature profile technique with a modified-Wilson plot to obtain the heating fluid's heat transfer coefficient in the annulus, wall thermocouples are not necessary either. Furthermore, wrapping a wire helically on the outside of the tube increases the water-side coefficient and promotes mixing that minimizes temperature gradients in the hot fluid from the top to the bottom of the annulus that can arise in stratified flow boiling test conditions.

10.6 Subcooled Boiling Heat Transfer

Subcooled flow boiling occurs when the local wall temperature during the heating of a subcooled liquid is above the saturation temperature of the fluid and sufficiently high for nucleation to occur. Subcooled boiling is characterized by vapor formation at the heated wall as isolated bubbles or as a bubbly layer along the wall. The bubbles are swept into the subcooled core by the liquid and then condense.

Gungor and Winterton (1986) have adapted their correlation to predict local heat transfer coefficients in the subcooled boiling regime by using separate temperature differences for driving the respective nucleate boiling and convective boiling processes. Thus, the heat flux is calculated as a sum of their two contributions as:

$$q = \alpha_L \left(T_w - T_L \right) + S\alpha_{nb} \left(T_{wall} - T_{sat} \right)$$
[10.6.1]

This predicted their database with a mean error of ±25%. Analogously, the other methods presented earlier for saturated forced convective evaporation in plain tubes may be adapted to estimate performance in subcooled flow boiling.